

## Differential Activation of Intracellular versus Plasmalemmal CB<sub>2</sub> Cannabinoid Receptors

G. Cristina Brailoiu,<sup>†</sup> Elena Deliu,<sup>‡</sup> Jahan Marcu,<sup>‡,§</sup> Nicholas E. Hoffman,<sup>||</sup> Linda Console-Bram,<sup>‡</sup> Pingwei Zhao,<sup>‡,§</sup> Muniswamy Madesh,<sup>||</sup> Mary E. Abood,<sup>\*,‡,§</sup> and Eugen Brailoiu<sup>\*,‡,||</sup>

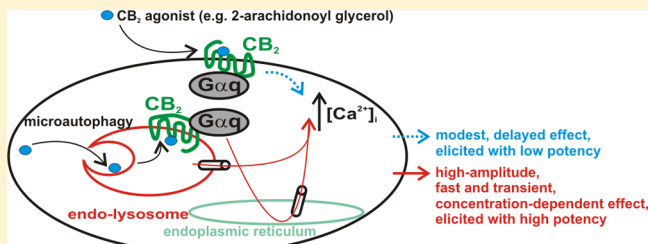
<sup>†</sup>Department of Pharmaceutical Sciences, Thomas Jefferson University School of Pharmacy, Philadelphia, Pennsylvania 19107, United States

<sup>‡</sup>Center for Substance Abuse Research, <sup>§</sup>Department of Anatomy and Cell Biology, <sup>||</sup>Center for Translational Medicine, and

<sup>\*</sup>Department of Pharmacology, Temple University School of Medicine, Philadelphia, Pennsylvania 19140, United States

### Supporting Information

**ABSTRACT:** The therapeutic and psychoactive properties of cannabinoids have long been recognized. The type 2 receptor for cannabinoids (CB<sub>2</sub>) has emerged as an important therapeutic target in several pathologies, as it mediates beneficial effects of cannabinoids while having little if any psychotropic activity. Difficulties associated with the development of CB<sub>2</sub>-based therapeutic agents have been related to its intricate pharmacology, including the species specificity and functional selectivity of the CB<sub>2</sub>-initiated responses. We postulated that a plasmalemmal or subcellular location of the receptor may contribute to the differential signaling pathways initiated by its activation. To differentiate between these two, we used extracellular and intracellular administration of CB<sub>2</sub> ligands and concurrent calcium imaging in CB<sub>2</sub>-expressing U2OS cells. We found that extracellular administration of anandamide was ineffective, whereas 2-arachidonoyl glycerol (2-AG) and WIN55,212-2 triggered delayed, CB<sub>2</sub>-dependent Ca<sup>2+</sup> responses that were Gq protein-mediated. When microinjected, all agonists elicited fast, transient, and dose-dependent elevations in intracellular Ca<sup>2+</sup> concentration upon activation of Gq-coupled CB<sub>2</sub> receptors. The CB<sub>2</sub> dependency was confirmed by the sensitivity to AM630, a selective CB<sub>2</sub> antagonist, and by the unresponsiveness of untransfected U2OS cells to 2-AG, anandamide, or WIN55,212-2. Moreover, we provide functional and morphological evidence that CB<sub>2</sub> receptors are localized at the endolysosomes, while their activation releases Ca<sup>2+</sup> from inositol 1,4,5-trisphosphate-sensitive- and acidic-like Ca<sup>2+</sup> stores. Our results support the functionality of intracellular CB<sub>2</sub> receptors and their ability to couple to Gq and elicit Ca<sup>2+</sup> signaling. These findings add further complexity to CB<sub>2</sub> receptor pharmacology and argue for careful consideration of receptor localization in the development of CB<sub>2</sub>-based therapeutic agents.



Although cannabinoids are active at several G protein-coupled receptors and ion channels, only two “true” cannabinoid receptors are recognized, namely CB<sub>1</sub> and CB<sub>2</sub>.<sup>1</sup> Interest in the latter has sparked as it appeared as an important therapeutic target in inflammatory and painful conditions,<sup>2,3</sup> while not being involved in the psychoactive cannabinoid effects, which are mainly CB<sub>1</sub>-mediated. As such, increasing effort is being spent in the development of CB<sub>2</sub>-based therapeutic agents.<sup>4,5</sup> Nonetheless, controversies exist, for instance, in CB<sub>2</sub> pharmacology and distribution.<sup>6–8</sup> At least two CB<sub>2</sub> receptor isoforms have been identified, with tissue- and species-specific expression patterns.<sup>8,9</sup> It has been found that CB<sub>2</sub> agonists may elicit distinct responses at CB<sub>2</sub> receptors from different species.<sup>10</sup> Moreover, functional selectivity, defined as the ability of a receptor to couple to different signaling pathways depending on the ligand that stimulates it,<sup>11</sup> has been reported for CB<sub>2</sub>.<sup>7</sup> Further complexity is added to the CB<sub>2</sub> receptor pharmacology with the recent finding that their intracellular activation modulates neuronal function.<sup>12</sup> Because CB<sub>2</sub> receptors have been found to signal through Ca<sup>2+</sup>,<sup>12–15</sup> we

used calcium imaging and extracellular and intracellular administration of cannabinoid ligands to investigate the functionality of plasmalemmal versus intracellular CB<sub>2</sub> receptors in U2OS cells stably expressing CB<sub>2</sub>.

### EXPERIMENTAL PROCEDURES

**Chemicals.** Anandamide, AM630, WIN55,212-2, 2-arachidonoyl glycerol (2-AG), and d-[Trp<sup>7,9,10</sup>]-substance P were obtained from Tocris Bioscience (R&D Systems, Minneapolis, MN). All other chemicals were from Sigma (St. Louis, MO).

**Cell Culture.** The CB<sub>2</sub>-β-arrestin2-GFP-U2OS (CB<sub>2</sub>-U2OS) cell line was kindly provided by M. Caron and L. S. Barak (Duke University, Durham, NC); the CB<sub>2</sub> receptor sequence is the CNR2\_Human sequence (GenBank accession code P34972). CB<sub>2</sub>-U2OS cells were maintained in DMEM supplemented with 10% fetal bovine serum, 100 mg/mL

Received: May 23, 2014

Revised: July 13, 2014

Published: July 17, 2014

Zeocin, and 200  $\mu$ g/mL G418 at 37 °C in a humidified incubator with 5% CO<sub>2</sub>. The serum was removed 24 h prior to experimentation. In experiments that aimed to evaluate Gq-dependent signaling, cell starvation was concomitant with incubation of d-[Trp7,9,10]-substance P (24 h).

**Immunocytochemistry and Confocal Imaging Studies.** U2OS cells transiently transfected with the GFP-tagged CB<sub>2</sub> receptor (kindly provided by M. Caron and L. S. Barak) and with Rab7-RFP (Addgene, Cambridge, MA) 48 h earlier were fixed with 4% paraformaldehyde, washed in phosphate-buffered saline, and mounted with DAPI Fluoromont G (Southern Biotech, Birmingham, AL). Cells were imaged using a Carl Zeiss 710 two-photon confocal microscope with a 63× oil immersion objective, using a 1× digital zoom, with excitations set for DAPI, GFP, and DsRed at 405, 488, and 561 nm, respectively. Images were analyzed using Zen 2010 (Zeiss), as previously reported.<sup>16</sup>

**Calcium Imaging.** Measurements of [Ca<sup>2+</sup>]<sub>i</sub> were performed as previously described.<sup>16–19</sup> Briefly, cells were incubated with 5  $\mu$ M Fura-2 AM (Invitrogen) in HBSS at room temperature for 45 min, washed with dye-free HBSS, and incubated for an additional 45 min to allow dye deesterification. Coverslips were mounted in an open bath chamber (RP-40LP, Warner Instruments, Hamden, CT) on the stage of an inverted microscope (Nikon Eclipse TiE, Nikon Inc., Melville, NY), equipped with a Perfect Focus System and a Photometrics CoolSnap HQ2 CCD camera (Photometrics, Tucson, AZ). During the experiments, the Perfect Focus System was activated. Fura-2 AM fluorescence (emission at 510 nm), following alternate excitation at 340 and 380 nm, was acquired at a frequency of 0.25 Hz. Images were acquired and analyzed using NIS-Elements AR version 3.1 (Nikon Inc.). After appropriate calibration with ionomycin and CaCl<sub>2</sub>, and Ca<sup>2+</sup>-free and EGTA, respectively, the ratio of the fluorescence signals (340 nm to 380 nm) was converted to Ca<sup>2+</sup> concentration.<sup>20</sup>

**Intracellular Microinjection.** Injections were performed using Femtotips II, InjectMan NI2, and FemtoJet systems (Eppendorf) as previously reported.<sup>16–19</sup> Pipettes were back-filled with an intracellular solution containing 110 mM KCl, 10 mM NaCl, and 20 mM HEPES (pH 7.2) or the compounds to be tested. The injection time was 0.4 s at 60 hectoPascal with a compensation pressure of 20 hectoPascal to ensure that the microinjected volume was <1% of the cell volume. The intracellular concentration of chemicals was determined on the basis of the concentration in the pipet and the volume of injection. The cells to be injected were Z-scanned before injection, and the cellular volume was automatically calculated by NIS-Elements AR version 3.1 (Nikon Inc.).

**Statistics.** Data are expressed as means and the standard error of the mean. One-way analysis of variance, followed by post hoc Bonferroni and Tukey tests, was used to assess significant differences between groups;  $P < 0.05$  was considered statistically significant.

## RESULTS

**Effects of Extracellular versus Intracellular Administration of CB<sub>2</sub> Agonist 2-Arachidonoyl Glycerol on the Cytosolic Ca<sup>2+</sup> Concentration of CB<sub>2</sub>-Expressing U2OS Cells.** We evaluated the Ca<sup>2+</sup> response of U2OS cells stably expressing the CB<sub>2</sub> receptor to bath application and intracellular microinjection of the endocannabinoid 2-arachidonoyl glycerol (2-AG). Increasing concentrations of 2-AG (0.01, 0.1,

and 1  $\mu$ M) were applied extracellularly to CB<sub>2</sub>-U2OS cells, which elevated the intracellular Ca<sup>2+</sup> concentration, [Ca<sup>2+</sup>]<sub>i</sub>, by 7 ± 3.4 nM ( $n = 31$  cells), 12 ± 5.1 nM ( $n = 43$  cells), and 87 ± 3.1 nM ( $n = 56$  cells), respectively (Figure 1A). The effect of

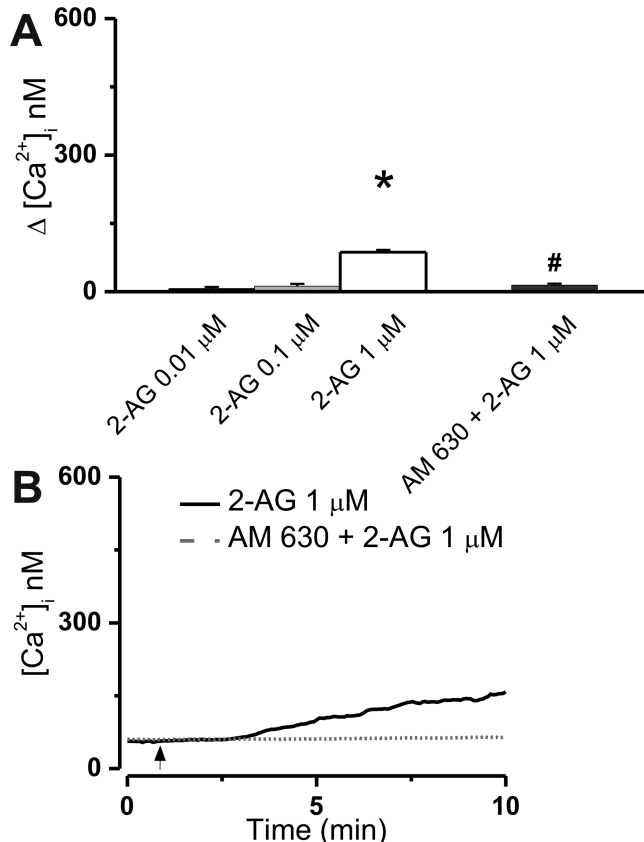


**Figure 1.** Extracellular administration of 2-arachidonoyl glycerol (2-AG) to CB<sub>2</sub>-U2OS cells elevates [Ca<sup>2+</sup>]<sub>i</sub>. (A) Comparison of the increases in [Ca<sup>2+</sup>]<sub>i</sub> produced by extracellular administration of 2-AG (0.01–1  $\mu$ M) and 1  $\mu$ M 2-AG in the presence of CB<sub>2</sub> receptor antagonist AM630 (1  $\mu$ M);  $P < 0.05$  compared with basal levels (\*) or with 1  $\mu$ M 2-AG (#). (B) Representative recordings of increases in [Ca<sup>2+</sup>]<sub>i</sub> in response to 1  $\mu$ M 2-AG in absence or presence of 1  $\mu$ M CB<sub>2</sub> antagonist AM630.

the latter concentration of 2-AG was statistically significant ( $P < 0.05$ ) and sensitive to CB<sub>2</sub> blockade with AM630 (1  $\mu$ M, 10 min). In the presence of AM630,  $\Delta[Ca^{2+}]_i$  was reduced to 14 ± 3.6 nM ( $n = 49$ ) (Figure 1A,B). The effect of 2-AG on [Ca<sup>2+</sup>]<sub>i</sub> was delayed by 1–2 min and increased gradually (Figure 1B).

In experiments using the intracellular microinjection technique, injection of 0.01, 0.1, and 1  $\mu$ M 2-AG (final concentrations inside the cell) induced robust and significant increases in [Ca<sup>2+</sup>]<sub>i</sub> of CB<sub>2</sub>-U2OS cells of 264 ± 11 nM ( $n = 6$  cells), 653 ± 19 nM ( $n = 6$  cells), and 938 ± 22 nM ( $n = 6$  cells), respectively, while control buffer microinjection had an insignificant effect of 49 ± 4 nM ( $n = 6$  cells) (Figure 2A–D). In the presence of co-injected CB<sub>2</sub> antagonist AM630 (1  $\mu$ M), 0.1  $\mu$ M 2-AG elevated [Ca<sup>2+</sup>]<sub>i</sub> by 58 ± 4 nM ( $n = 6$  cells), similar to that of control buffer microinjection; the effect of 0.1  $\mu$ M 2-AG on [Ca<sup>2+</sup>]<sub>i</sub> of untransfected U2OS cells was also insignificant, measuring 34 ± 5 nM ( $n = 6$  cells) (Figure 2A,B,E,F).

In all series of experiments using intracellular injection, CB<sub>2</sub>-U2OS cells were pretreated for 1 min with 1  $\mu$ M AM630

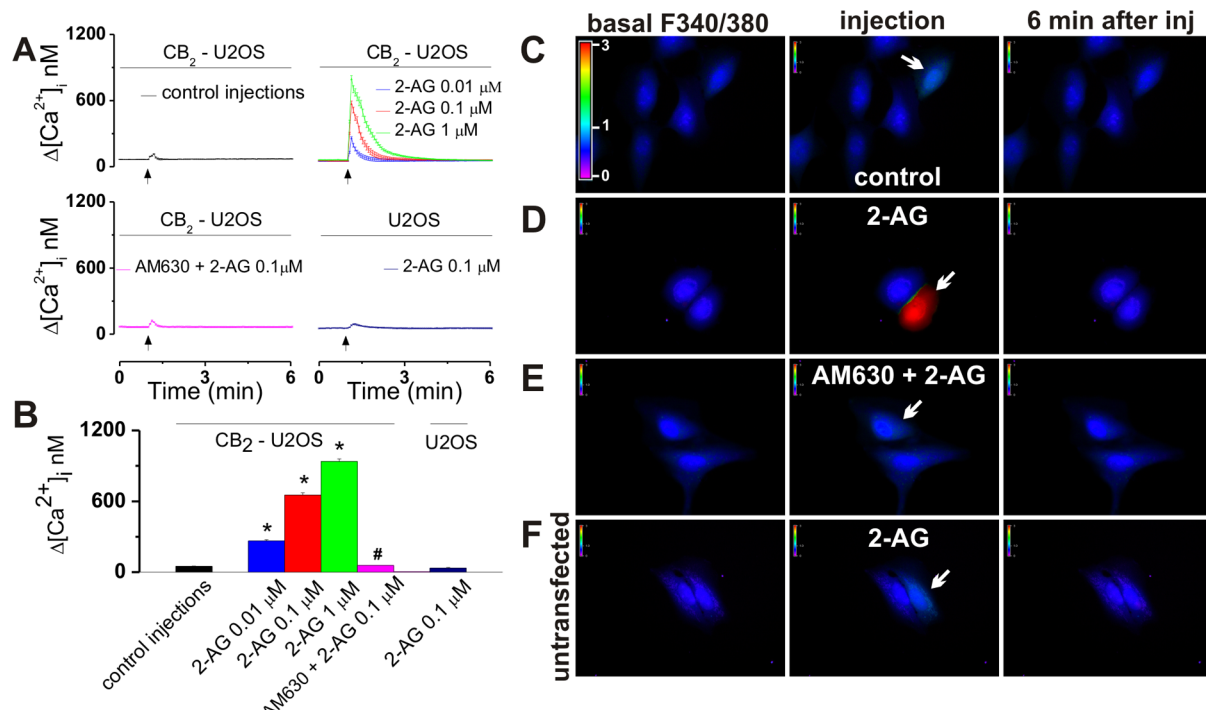


**Figure 2.** Intracellular microinjection of 2-AG into CB<sub>2</sub>-U2OS cells produces CB<sub>2</sub>-dependent Ca<sup>2+</sup> elevation. (A) Averaged increases in [Ca<sup>2+</sup>]<sub>i</sub> produced by intracellular administration of control buffer (top left) or 2-AG (0.01, 0.1, and 1 μM, final concentrations inside the cell, top right), co-injection of 0.1 μM 2-AG with CB<sub>2</sub> antagonist AM630 (1 μM, bottom left) in CB<sub>2</sub>-U2OS cells, or microinjection of 0.1 μM 2-AG into control U2OS cells (bottom right). (B) Comparison of the Ca<sup>2+</sup> responses elicited by the treatments of CB<sub>2</sub>-U2OS or control untransfected U2OS cells mentioned above; *P* < 0.05 when compared with the control (\*) or with 2-AG alone (#). (C–F) Characteristic fluorescence images of Fura-2 AM-loaded CB<sub>2</sub>-U2OS cells before (left), during (middle), and 6 min after (right) intracellular administration of control buffer (C), 0.1 μM 2-AG alone (D), or 0.1 μM 2-AG in the presence of 1 μM AM630 (E) or of U2OS cells treated with 0.1 μM 2-AG (F). Arrows denote the injected cells; the fluorescence scale (0–3) is illustrated in each panel and magnified in the left panel of part C.

(applied extracellularly), to exclude the possibility that the injected cannabinoid ligands leaked from the pipet and triggered plasma membrane receptor-mediated effects.

**Functional and Morphological Evidence of Localization of CB<sub>2</sub> to Endolysosomes in CB<sub>2</sub>-Transfected U2OS Cells.** CB<sub>2</sub>-U2OS cells were incubated for 1 h with either 1 μM bafilomycin A1, a V-type ATPase that prevents lysosomal acidification,<sup>21</sup> or 30 μM rapamycin, which blocks the last step of the engulfment of molecules by endolysosomes via microautophagy.<sup>22</sup> Under the conditions described above, the effect of 0.1 μM 2-AG on [Ca<sup>2+</sup>]<sub>i</sub>, initially measuring 653 ± 19 nM, was drastically reduced to 36 ± 4.8 nM (*n* = 6 cells) and 67 ± 9.1 nM (*n* = 6 cells) (Figure 3A–E). In U2OS cells co-expressing GFP-tagged CB<sub>2</sub> receptors and RFP-tagged Rab7, a small GTPase associated with both endosomes and lysosomes,<sup>23</sup> we observed an extensive colocalization of CB<sub>2</sub> and Rab7 (Figure 3F). Lysosomal disruption using bafilomycin A1 greatly reduced the extent of the merged signal of CB<sub>2</sub> and Rab7 (Figure 3F).

**Intracellular, but Not Extracellular, Administration of Anandamide Elevates the Cytosolic Ca<sup>2+</sup> Concentration of CB<sub>2</sub>-Expressing U2OS Cells.** CB<sub>2</sub>-U2OS cells extracellularly treated with progressive concentrations of anandamide (0.01, 0.1, and 1 μM) failed to respond with a significant increase in [Ca<sup>2+</sup>]<sub>i</sub> (Figure 1 of the Supporting Information); incubation with CB<sub>2</sub> antagonist AM630 (1 μM) did not modify the response to 1 μM anandamide (Figure 1 of the Supporting Information).

However, CB<sub>2</sub>-U2OS cells responded to intracellular administration of anandamide (0.01, 0.1, and 1 μM, final concentrations inside the cell) with significant and concentration-dependent elevations of [Ca<sup>2+</sup>]<sub>i</sub>: 124 ± 7.4, 368 ± 8.4, and 574 ± 7.2 nM, respectively [*n* = 6 cells for each concentration tested (Figure 4A,B)]. The anandamide-induced increase in [Ca<sup>2+</sup>]<sub>i</sub> was fast and transient (Figure 4A); blockade of intracellular CB<sub>2</sub> receptors upon co-injection of 1 μM AM630 prevented the effect of microinjected anandamide (1 μM), reducing it to 37 ± 4.1 nM [*n* = 6 cells (Figure 4A–D)], a response similar to that elicited by control buffer microinjection (Figure 2). Characteristic images depicting the increases in the Fura-2 fluorescence ratio at 340 and 380 nm upon microinjection of anandamide (1 μM) in the absence or presence of AM630 (1 μM) are shown in panels C and D of Figure 4.

Anandamide produced negligible effects in control untransfected U2OS cells regardless of whether it was applied extracellularly (Figure 2 of the Supporting Information) or intracellularly (Figure 3 of the Supporting Information).

**WIN55,212-2 Produces CB<sub>2</sub> Receptor-Dependent Increases in Ca<sup>2+</sup> Concentration in CB<sub>2</sub>-U2OS Cells.** Extracellular administration of WIN55,212-2 (0.01, 0.1, and 1 μM) elevated [Ca<sup>2+</sup>]<sub>i</sub> by 11 ± 8.1 nM (*n* = 27 cells), 17 ± 6.3 nM (*n* = 38 cells), and 262 ± 6.8 nM [*n* = 46 cells (Figure 5A,B)]; the latter effect was statistically significant (*P* < 0.05) and sensitive to CB<sub>2</sub> blockade with AM630 [1 μM, incubation for 10 min, Δ[Ca<sup>2+</sup>]<sub>i</sub> reduced to 12 ± 6.8 nM (*n* = 36 cells)] (Figure 5A,B). The Ca<sup>2+</sup> response elicited by WIN55,212-2

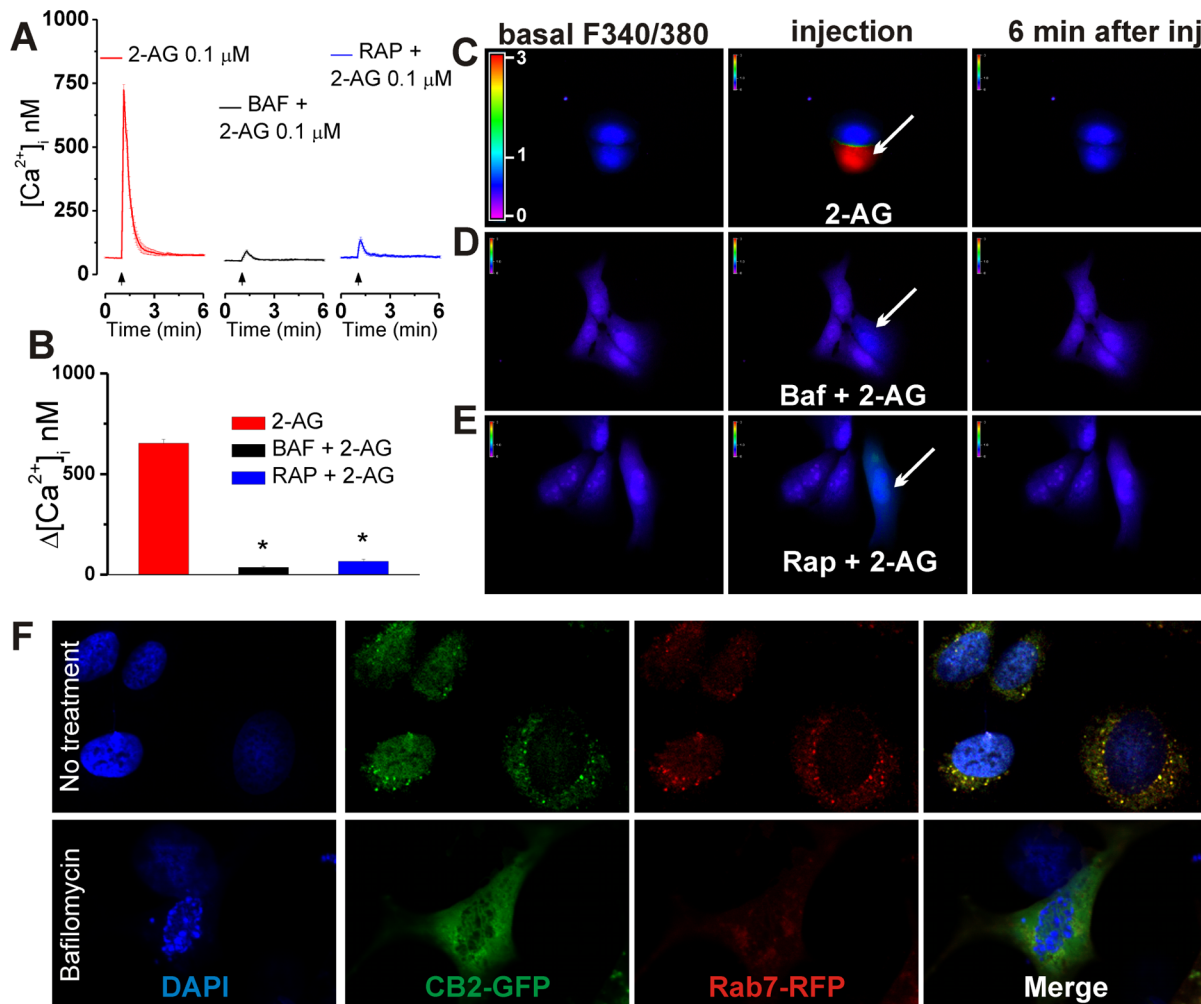


**Figure 3.** Intracellular CB<sub>2</sub> receptors are located at endolysosomes in CB<sub>2</sub>-expressing U2OS cells. (A) Averaged Ca<sup>2+</sup> responses of CB<sub>2</sub>-U2OS cells to intracellular administration of 0.1  $\mu$ M 2-AG in the absence (left) or presence of lysosomal disruptor baflomycin A1 (1  $\mu$ M, incubation for 1 h, middle) or microautophagy inhibitor rapamycin (30  $\mu$ M, incubation for 1 h, right). (B) Comparison of the increases in [Ca<sup>2+</sup>]<sub>i</sub> elicited by 2-AG under the conditions described above;  $P < 0.05$  when compared with 2-AG microinjection (\*). (C–E) Representative fluorescence images of Fura-2 AM-loaded CB<sub>2</sub>-U2OS cells before (left), during (middle), and 6 min after (right) intracellular administration of 0.1  $\mu$ M 2-AG in the absence (C) and presence of baflomycin A1 (D) or rapamycin (E). (F) Confocal images (top row) showing the colocalization of the GFP-tagged CB<sub>2</sub> receptor and RFP-tagged Rab7, an endolysosomal marker, in GFP-CB<sub>2</sub>- and RFP-Rab7-transfected U2OS cells; the nuclei are labeled with DAPI (blue). Lysosomal disruption (bottom row) with baflomycin A1 markedly reduces the extent of the merged immunostaining of CB<sub>2</sub> and Rab7.

occurred with a latency of 1–2 min (Figure 5B), similar to the effect of bath-applied 2-AG (Figure 1B).

Microinjection of WIN55,212-2 (0.01, 0.1, and 1  $\mu$ M, final concentrations inside the cell) into CB<sub>2</sub>-U2OS cells triggered fast, transient, and concentration-dependent increases in [Ca<sup>2+</sup>]<sub>i</sub> of 257  $\pm$  5.3, 635  $\pm$  7.1, and 924  $\pm$  17 nM ( $n = 6$  cells for each concentration tested), whereas when 1  $\mu$ M AM630 was co-injected with 1  $\mu$ M WIN55,212-2, a small and insignificant increase in Ca<sup>2+</sup> concentration, of 31  $\pm$  4.6 nM ( $n = 6$  cells), was apparent (Figure 6A,B). Representative examples of the increase in the F<sub>340</sub>/F<sub>380</sub> fluorescence ratio produced by intracellular administration of WIN55,212-2 or AM630 and WIN55,212-2 are shown in panels C and D of Figure 6. The insignificant Ca<sup>2+</sup> responses to extracellular and intracellular administration of WIN55,212-2 in control U2OS cells are illustrated in Figures 2 and 3 of the Supporting Information, respectively.

#### Effects of Extracellular 2-AG and WIN55,212-2 Are Mediated by Gq Coupling of CB<sub>2</sub> Receptors.

2-AG (1  $\mu$ M), anandamide (1  $\mu$ M), or WIN55,212-2 (1  $\mu$ M) was bath-applied to CB<sub>2</sub>-U2OS cells treated overnight with chemicals interfering with G protein signaling. After cholera toxin (CTX, 100 ng/mL) pretreatment, 2-AG produced an increase in the [Ca<sup>2+</sup>]<sub>i</sub> of 83  $\pm$  5.1 nM [ $n = 61$  cells (Figure 7A,B)] similar to the effect of 2-AG on untreated cells. CTX irreversibly abolishes the GTPase activity of the Gs  $\alpha$  subunit, inducing continual activation of adenylyl cyclase and increased intracellular levels of cAMP. In this manner, it hinders ligands of Gs-coupled receptors from eliciting their Gs-dependent effects. After pretreatment with the Gi/o inhibitor pertussis toxin (PTX, 100 ng/mL), the response of 2-AG was negligibly modified, measuring 85  $\pm$  4.2 nM [ $n = 53$  cells (Figure 7A,B)]. Conversely, pretreatment of CB<sub>2</sub>-U2OS cells with Gq blocker d-[Trp7,9,10]-substance P (D-SP, 100 ng/mL)<sup>24</sup> greatly reduced the effect of 2-AG to 7  $\pm$  2.7 nM [ $n = 67$  cells (Figure 7A,B)].

The Ca<sup>2+</sup> response elicited by anandamide was largely similar and not significant regardless of whether anandamide was

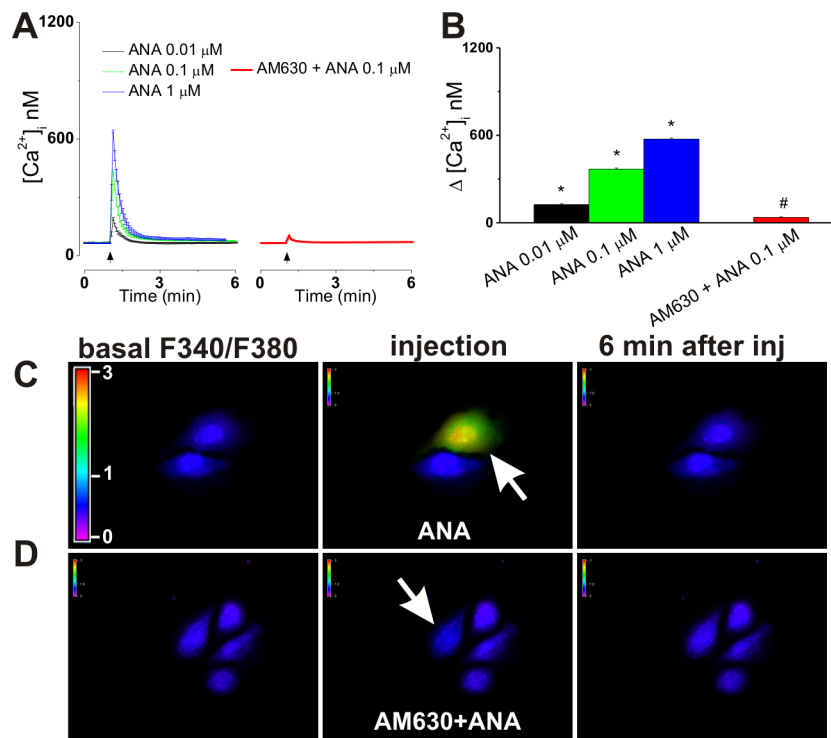


**Figure 4.** Intracellular administration of anandamide increases  $[Ca^{2+}]_i$  in CB<sub>2</sub>-U2OS cells. (A) Averaged  $Ca^{2+}$  responses induced by increasing doses of microinjected anandamide (ANA, 0.01–1  $\mu M$ , left) or by co-injection of 0.1  $\mu M$  anandamide and 1  $\mu M$  CB<sub>2</sub> antagonist AM630 (right). (B) Comparison of the increases in  $[Ca^{2+}]_i$  produced by microinjected anandamide (0.01, 0.1, and 1  $\mu M$ ) and anandamide (0.1  $\mu M$ ) in the presence of AM630 (1  $\mu M$ ).  $P < 0.05$  compared with the control (\*) or with 0.1  $\mu M$  anandamide alone (#). (C and D) Typical fluorescence images of Fura-2 AM-loaded CB<sub>2</sub>-U2OS cells before (left), during (middle), and 6 min after (right) intracellular administration of 0.1  $\mu M$  anandamide alone (C) or in the presence of 1  $\mu M$  AM630 (D). Arrows denote the injected cells; the fluorescence scale (0–3) is illustrated in each panel and magnified in the left panel of part C.

applied alone [ $\Delta [Ca^{2+}]_i$  of  $9 \pm 4.7$  nM ( $n = 33$  cells)] or after stimulating Gs-dependent signaling with CTX (100 ng/mL), inhibiting Gi/o with PTX (100 ng/mL), and inhibiting Gq with D-SP (100 ng/mL). The  $\Delta [Ca^{2+}]_i$  values were  $8 \pm 5.2$  nM ( $n = 29$  cells),  $6 \pm 4.8$  nM ( $n = 41$  cells), and  $7 \pm 2.3$  nM ( $n = 36$  cells), respectively (Figure 7A,B).

D-SP pretreatment drastically diminished the effect induced by WIN55,212-2, reducing it to  $58 \pm 3.9$  nM, while in the presence of CTX or PTX, WIN55,212-2 increased  $[Ca^{2+}]_i$  to similar extents as in their absence:  $\Delta [Ca^{2+}]_i$  values were  $257 \pm 6.8$  nM ( $n = 53$  cells) and  $243 \pm 7.9$  nM ( $n = 47$  cells) in cells pretreated with CTX and PTX, respectively, and  $262 \pm 6.8$  nM ( $n = 49$  cells) for WIN55,212-2 alone (Figure 7A,B).

**Intracellular CB<sub>2</sub> Receptors Couple to Gq Proteins.** Overnight treatment of CB<sub>2</sub>-U2OS cells with CTX (100 ng/mL) or PTX (100 ng/mL) failed to significantly modify the  $Ca^{2+}$  response elicited by intracellular administration of 0.1  $\mu M$  2-AG (Figure 8A,B). Under the conditions described above, 2-AG increased  $[Ca^{2+}]_i$  by  $654 \pm 21$  nM ( $n = 6$  cells) and  $629 \pm 18$  nM ( $n = 6$  cells), respectively, while the response to 2-AG alone measured  $652 \pm 19$  nM [ $n = 6$  cells (Figure 8A,B)]. After incubation of cells with D-SP (100 ng/mL), the effect of 2-AG was greatly decreased to  $62 \pm 23$  nM ( $n = 6$  cells), indicating participation of a Gq-dependent pathway in the response (Figure 8A,B).

Upon pretreatment with CTX (100 ng/mL) or PTX (100 ng/mL), intracellular injection of anandamide (0.1  $\mu M$ ) elevated  $[Ca^{2+}]_i$  of CB<sub>2</sub>-U2OS cells by  $359 \pm 7.2$  nM ( $n = 6$  cells) or  $355 \pm 11.2$  nM ( $n = 6$  cells), respectively; these effects are similar to those triggered by microinjected anandamide

alone [ $368 \pm 8.4$  nM ( $n = 6$  cells)], indicating that Gs and Gi/o proteins are not mediating its effect. Upon D-SP (100 ng/mL) pretreatment, intracellular anandamide produced an insignificant  $Ca^{2+}$  response of  $38 \pm 6.3$  nM [ $n = 6$  cells (Figure 8A,B)].

Similarly, CTX and PTX (both at 100 ng/mL) pretreatment did not significantly modify the response of CB<sub>2</sub>-U2OS cells to microinjected WIN55,212-2 (0.1  $\mu M$ ).  $\Delta [Ca^{2+}]_i$  values were  $668 \pm 13$  nM ( $n = 6$  cells) and  $641 \pm 9.8$  nM ( $n = 6$  cells) after CTX and after PTX, respectively, and  $635 \pm 7.1$  nM for WIN55,212-2 alone. However, blocking Gq proteins with 100 ng/mL D-SP basically abolished the effect of intracellular WIN55,212-2. In this case,  $\Delta [Ca^{2+}]_i$  decreased to  $27 \pm 5.4$  nM [ $n = 6$  cells (Figure 8A,B)].

**Activation of Intracellular CB<sub>2</sub> Mobilizes Ca<sup>2+</sup> from Distinct Pools.** CB<sub>2</sub>-U2OS cells incubated with Ca<sup>2+</sup>-free saline responded to microinjection of 0.1  $\mu M$  2-AG with a  $457 \pm 5.2$  nM increase in  $[Ca^{2+}]_i$  ( $n = 6$  cells), while the effect of control buffer microinjection was negligible [ $\Delta [Ca^{2+}]_i = 29 \pm 1.7$  nM [ $n = 6$  cells (Figure 9A,B)]]. The response to 2-AG was reduced in Ca<sup>2+</sup>-free versus Ca<sup>2+</sup>-containing HBSS [ $\Delta [Ca^{2+}]_i = 653 \pm 19$  nM (Figure 2)], indicating mobilization of both intracellular and extracellular Ca<sup>2+</sup> pools. Using a pharmacological approach, we further sought to identify the intracellular sources of Ca<sup>2+</sup> involved in the response to microinjected 2-AG. Pretreatment of cells with ryanodine receptor blocker ryanodine (10  $\mu M$ , 1 h) did not significantly modify the Ca<sup>2+</sup> response to 2-AG, which measured  $452 \pm 5.9$  nM [ $n = 6$  cells (Figure 9A,B)]. Conversely, pretreatment with Ned-19 (5  $\mu M$ , 15 min), which blocks endolysosomal Ca<sup>2+</sup> release via the NAADP-sensitive two-pore channels,<sup>25</sup> decreased the extent of

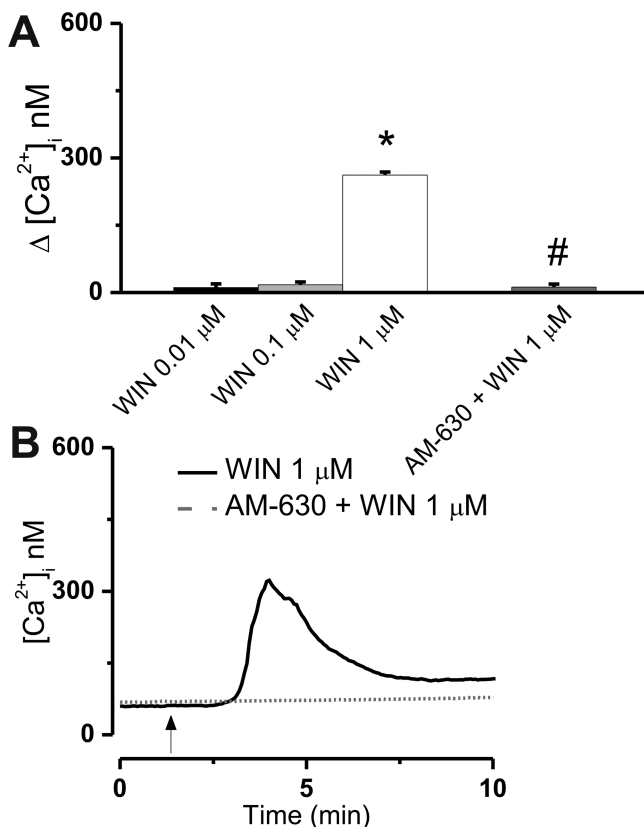


**Figure 5.** Extracellular administration of WIN55,212-2 to CB<sub>2</sub>-U2OS cells elevates [Ca<sup>2+</sup>]<sub>i</sub>. (A) Comparison of the increases in [Ca<sup>2+</sup>]<sub>i</sub> produced by extracellular administration of WIN55,212-2 (WIN, 0.01–1 μM) and 1 μM WIN55,212-2 in the presence of CB<sub>2</sub> receptor antagonist AM630 (1 μM);  $P < 0.05$  compared with basal levels (\*) or with 1 μM WIN55,212-2 (#). (B) Representative recordings of increases in [Ca<sup>2+</sup>]<sub>i</sub> in response to 1 μM WIN in the absence or presence of 1 μM CB<sub>2</sub> antagonist AM630.

the Ca<sup>2+</sup> elevation produced by 2-AG to  $349 \pm 4.3$  nM ( $n = 6$  cells); inositol 1,4,5-trisphosphate receptor (IP<sub>3</sub>R) inhibition induced by treating CB<sub>2</sub>-U2OS cells with heparin and xestospongin C (10 μM, 15 min) also induced a significant decrease in the response to 2-AG {Δ[Ca<sup>2+</sup>]<sub>i</sub> =  $168 \pm 3.6$  nM [ $n = 6$  cells (Figure 9A,B)]}. When both IP<sub>3</sub>Rs and the two-pore channels were blocked, the Ca<sup>2+</sup> response to intracellular microinjection of 2-AG was completely abolished {Δ[Ca<sup>2+</sup>]<sub>i</sub> =  $34 \pm 2.4$  nM [ $n = 6$  cells (Figure 9A,B)]}.

## ■ DISCUSSION

In addition to the effects initiated at the plasma membrane, G protein-coupled receptors (GPCRs) may also trigger signaling cascades upon their activation within the cell.<sup>26</sup> The emerging paradigm of functional intracellular GPCRs is particularly significant in the case of lipid messengers that are generated intracellularly and may target their receptors at both sites, (reviewed in ref 27). We and others reported the functionality of intracellularly expressed CB<sub>1</sub> receptors,<sup>17,28</sup> as well as their ability to use Ca<sup>2+</sup> as a second messenger.<sup>17</sup> To evaluate whether CB<sub>2</sub> receptors elicit Ca<sup>2+</sup> signaling upon plasmalemmal or intracellular activation, cannabinoid ligands were administered extracellularly or microinjected into U2OS cells stably expressing CB<sub>2</sub>.

We noticed that extracellular administration of 2-AG induced a small increase in [Ca<sup>2+</sup>]<sub>i</sub> of CB<sub>2</sub>-U2OS cells only at the

highest concentration tested here (1 μM). Bath application of anandamide did not elevate [Ca<sup>2+</sup>]<sub>i</sub> of CB<sub>2</sub>-U2OS cells. While 2-AG produced a gradual increase in [Ca<sup>2+</sup>]<sub>i</sub> of CB<sub>2</sub>-U2OS cells, a robust Ca<sup>2+</sup> response was induced by extracellular administration of WIN55,212-2, which is a cannabinoid agonist displaying high affinity and/or intrinsic activity at this receptor.<sup>1,29</sup> The CB<sub>2</sub> specificity was indicated by the ability of CB<sub>2</sub> antagonist AM630<sup>29</sup> to inhibit the effects of extracellular administration of 2-AG and WIN55,212-2 in CB<sub>2</sub>-U2OS cells and by the unresponsiveness of untransfected U2OS cells to bath application of WIN55,212-2.

Similar to CB<sub>1</sub>, CB<sub>2</sub> receptors couple to Gi proteins and inhibit cAMP formation or activate MAPK.<sup>6,29</sup> However, coupling to Gs or Gq of CB<sub>1</sub> receptors has also been reported.<sup>30,31</sup> While a cannabinoid-dependent [Ca<sup>2+</sup>]<sub>i</sub> increase may occur downstream of Gi,<sup>32,33</sup> we noticed that the CB<sub>2</sub>-dependent effects of 2-AG or WIN55,212-2 were completely contingent on Gq in our paradigm. WIN55,212-2 also activates Gq downstream of CB<sub>1</sub>,<sup>31</sup> moreover, it can trigger a CB<sub>2</sub>-dependent signaling pathway different from that elicited by other ligands.<sup>7</sup> Thus, the discrepancy between the effects of extracellular administration of anandamide, 2-AG, and WIN55,212-2 in our study may be a result of the reported functional selectivity at CB<sub>2</sub> receptors.<sup>7,34</sup>

In a recent study, we demonstrated that anandamide can trigger fast CB<sub>1</sub>-dependent Ca<sup>2+</sup> signaling upon microinjection but is ineffective upon extracellular administration in CB<sub>1</sub>-transfected cells.<sup>17</sup> To test the hypothesis of functional intracellular CB<sub>2</sub> receptors in CB<sub>2</sub>-U2OS cells, intracellular injections of 2-AG, anandamide, or WIN55,212-2 were conducted. When 2-AG or anandamide was microinjected, concentration-dependent elevations of [Ca<sup>2+</sup>]<sub>i</sub> were observed, and the Ca<sup>2+</sup> response pattern was very fast, which is in contrast with the delayed, modest response and lack of effect, respectively, observed with the extracellular administration of these two agonists. Likewise, intracellular administration of WIN55,212-2 resulted in a concentration-dependent and robust effect. WIN55,212-2 and 2-AG produced Ca<sup>2+</sup> responses with an amplitude higher than that of anandamide, which is consistent with the full agonistic activity at CB<sub>2</sub> receptors reported for these ligands.<sup>1,29</sup> The sensitivity of these responses to the intracellular blockade of CB<sub>2</sub> and the unresponsiveness of control, untransfected U2OS cells to microinjected cannabinoids were considered to be indicative of CB<sub>2</sub> specificity. We further noticed that interfering with Gq-dependent, but not with Gs- or Gi/o-dependent, signaling prevented the effect of microinjected 2-AG, anandamide, or WIN55,212-2. Moreover, the endocannabinoids and WIN55,212-2 trigger similar signaling pathways upon intracellular administration, despite their unrelated chemical structure.

The accumulating evidence pointing to endolysosomes as intracellular locations where GPCRs initiate signaling<sup>16,18,19,35,36</sup> prompted us to evaluate whether this may be the case for CB<sub>2</sub>. In an initial functional study, we found that the effect of intracellular 2-AG is abolished by lysosomal disruption. Because rapamycin reduced the effects of microinjected 2-AG, ligand microautophagy<sup>22</sup> may be a necessary step in the activation of endolysosomally located CB<sub>2</sub>. The localization of CB<sub>2</sub> to lysosomes was confirmed by an additional study, providing morphological evidence that CB<sub>2</sub> colocalizes with the endolysosomal-associated small GTPase Rab7. Lysosomal disruption with bafilomycin A1 markedly

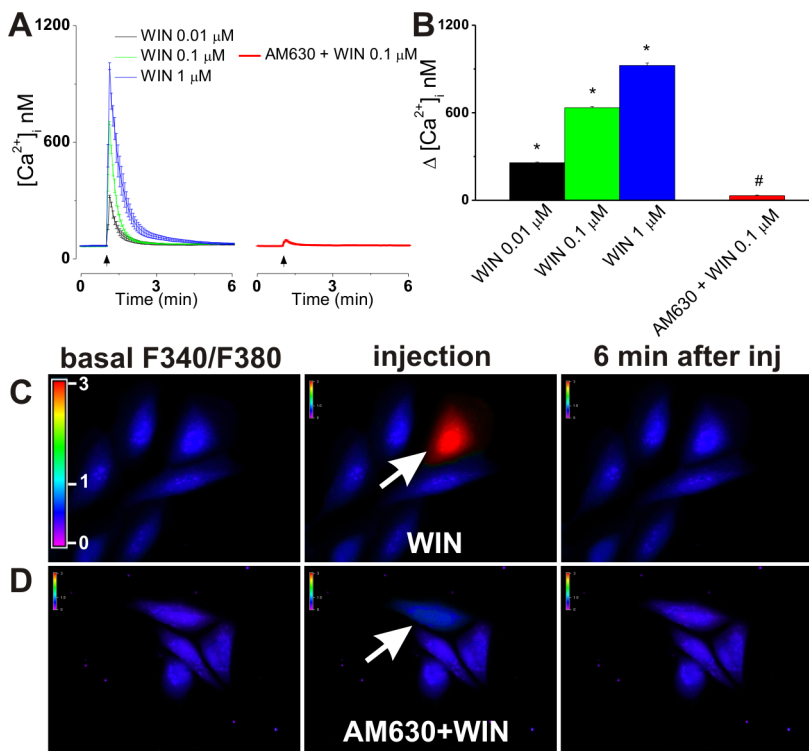


**Figure 6.** Microinjection of WIN55,212-2 increases  $[\text{Ca}^{2+}]_i$  in CB<sub>2</sub>-U2OS cells. (A) Averaged  $[\text{Ca}^{2+}]_i$  elevations produced by increasing doses of microinjected WIN55,212-2 (WIN 0.01–1  $\mu\text{M}$ , left) or by co-injection of 0.1  $\mu\text{M}$  WIN55,212-2 and 1  $\mu\text{M}$  CB<sub>2</sub> antagonist AM630 (right). (B) Comparison of the increases in  $[\text{Ca}^{2+}]_i$  elicited by microinjected WIN55,212-2 (0.01, 0.1, and 1  $\mu\text{M}$ ) and WIN55,212-2 (0.1  $\mu\text{M}$ ) in the presence of AM630 (1  $\mu\text{M}$ );  $P < 0.05$  compared with the control (\*) (see Figure 2) or with 0.1  $\mu\text{M}$  WIN55,212-2 alone (#). (C and D) Characteristic fluorescence images of Fura-2 AM-loaded CB<sub>2</sub>-U2OS cells before (left), during (middle), and 6 min after (right) intracellular administration of 0.1  $\mu\text{M}$  WIN55,212-2 alone (C) or in the presence of 1  $\mu\text{M}$  AM630 (D). Arrows denote the injected cells; the fluorescence scale (0–3) is illustrated in each panel and magnified in the left panel of part C.

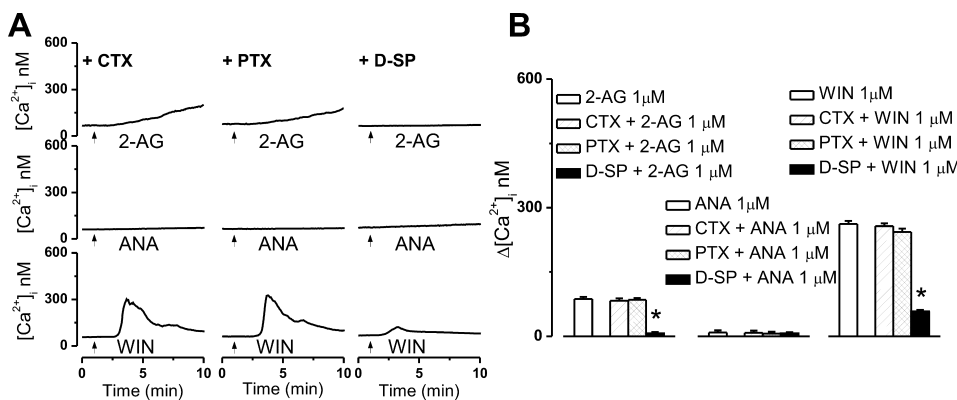


**Figure 7.** The  $\text{Ca}^{2+}$  responses produced by bath-applied 2-AG and WIN55,212-2 are prevented by a Gq protein inhibitor. (A) Representative examples of the  $\text{Ca}^{2+}$  responses induced by 1  $\mu\text{M}$  2-AG (top), 1  $\mu\text{M}$  anandamide (ANA, middle), or 1  $\mu\text{M}$  WIN55,212-2 (WIN, bottom), applied by bath to CB<sub>2</sub>-expressing U2OS cells in the presence of cholera toxin (CTX, 100 nM, top), which occludes Gs-dependent signaling, Gi/o blocker pertussis toxin (PTX, 100 nM, middle), or Gq protein inhibitor D-[Trp7,9,10]-substance P (D-SP, 100  $\mu\text{M}$ , bottom); 2-AG and WIN55,212-2 increased  $[\text{Ca}^{2+}]_i$ , and the response was Gq protein-mediated. (B) Comparison of the mean amplitude of the  $\text{Ca}^{2+}$  responses produced by extracellular administration of 1  $\mu\text{M}$  2-AG (left), 1  $\mu\text{M}$  anandamide (middle), or 1  $\mu\text{M}$  WIN55,212-2 (right) in the absence and presence of the indicated G protein inhibitors;  $P < 0.05$  compared with WIN55,212-2 alone (\*).

reduced the fluorescence intensity of both CB<sub>2</sub> and Rab7, supporting the findings of the functional study.

Next, we sought to examine the pools of  $\text{Ca}^{2+}$  mobilized upon activation of intracellularly located CB<sub>2</sub>. The reduction in the amplitude of the  $\text{Ca}^{2+}$  response of CB<sub>2</sub>-U2OS cells incubated with  $\text{Ca}^{2+}$ -free saline to microinjected 2-AG indicated that both influx of extracellular  $\text{Ca}^{2+}$  and release of  $\text{Ca}^{2+}$  from intracellular stores occur downstream of intracellular CB<sub>2</sub>

activation. Using a pharmacological approach, we further determined that 2-AG-induced stimulation of intracellular CB<sub>2</sub> results in  $\text{Ca}^{2+}$  mobilization from endolysosomes via NAADP-sensitive two-pore channels and from the endoplasmic reticulum via the IP<sub>3</sub>R. This effect correlates well with the localization of CB<sub>2</sub> at the endolysosomes, as well as with the localization of NAADP-generating enzymes<sup>37,38</sup> at the membrane of acidic organelles.<sup>39</sup>

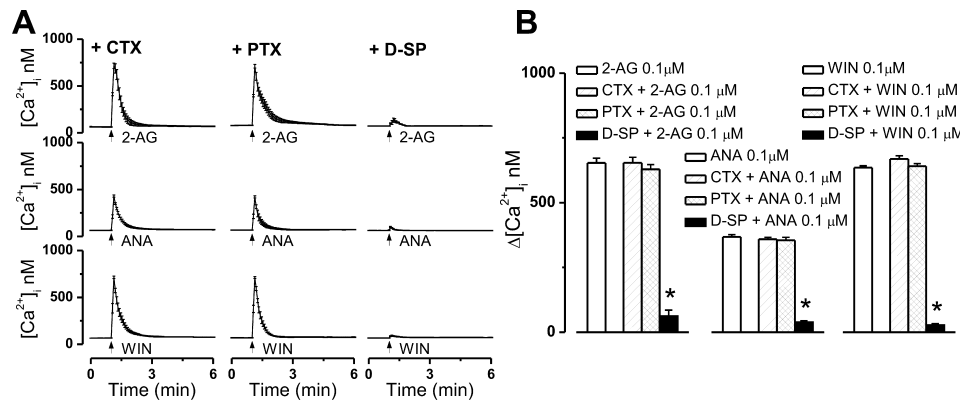


**Figure 8.** Intracellular microinjection of 2-AG, anandamide, or WIN55,212-2 produces Gq-dependent  $Ca^{2+}$  responses in CB<sub>2</sub>-expressing U2OS cells. (A) Averaged  $Ca^{2+}$  responses induced by intracellular administration of 0.1  $\mu$ M 2-AG (top), 0.1  $\mu$ M anandamide (ANA, middle), or 0.1  $\mu$ M WIN55,212-2 (WIN, bottom) in CB<sub>2</sub>-U2OS cells pretreated with cholera toxin (CTX, 100 nM, top), pertussis toxin (PTX, 100 nM, middle), or Gq protein inhibitor D-[Trp<sup>7,9,10</sup>]-substance P (D-SP, 100  $\mu$ M, bottom); each ligand increased  $[Ca^{2+}]_i$ , and the response was sensitive to Gq protein blockade. (B) Comparison of the mean amplitude of the  $Ca^{2+}$  responses produced by intracellular administration of 0.1  $\mu$ M 2-AG (left), 0.1  $\mu$ M anandamide (middle), or 0.1  $\mu$ M WIN55,212-2 (right) in absence and presence of the indicated G protein inhibitors; in each group of data,  $P < 0.05$  compared with 2-AG, anandamide, or WIN55,212-2 alone (\*).

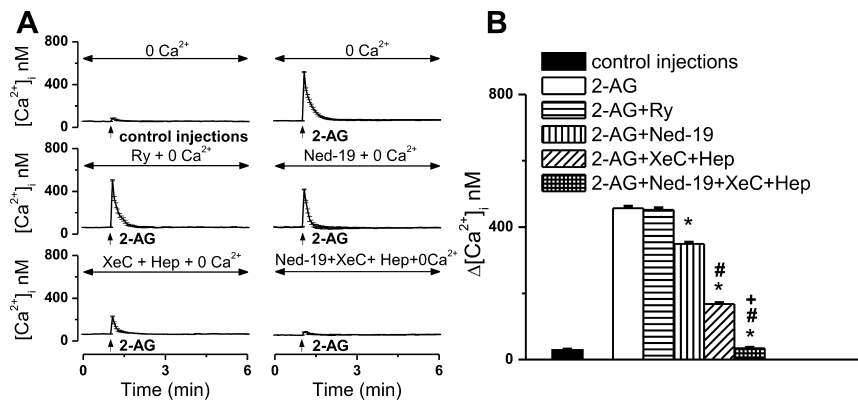


**Figure 9.** 2-AG mobilizes endoplasmic reticulum and acidic-like  $Ca^{2+}$  stores. (A) Averaged  $Ca^{2+}$  responses of CB<sub>2</sub>-U2OS cells in  $Ca^{2+}$ -free saline, microinjected with either control buffer or 0.1  $\mu$ M 2-AG in the absence or presence of ryanodine receptor blocker ryanodine (Ry), two-pore channel antagonist Ned-19, IP<sub>3</sub>R inhibitors xestospongin C (XeC) and heparin (Hep), or a combination of Ned-19, XeC, and Hep. (B) Comparison of the  $Ca^{2+}$  increases produced by the treatments described in (A);  $P < 0.05$  compared with 2-AG microinjection (\*), 2-AG in the presence of Ned-19 (#), or 2-AG in the presence of IP<sub>3</sub>R blockers (+).

Thus, we conclude that intracellular CB<sub>2</sub> receptors are functional, endolysosomally located, and Gq-coupled in CB<sub>2</sub>-U2OS cells, and their activation mobilizes NAADP-sensitive acidic-like  $Ca^{2+}$  stores and inositol 1,4,5-trisphosphate-sensitive endoplasmic reticulum pools. In addition, we note that CB<sub>2</sub> agonists elicit discrepant and delayed effects and exhibit a considerably lower potency when administered extracellularly as opposed to intracellularly. Although these effects appear to be Gq-mediated, it may be that a considerable pool of plasmalemmal CB<sub>2</sub> receptors do not couple with Gq/ $Ca^{2+}$  signaling. Conversely, Gq coupling and associated  $Ca^{2+}$  responses may be a characteristic of intracellularly located CB<sub>2</sub>, in which case the delay in the effects elicited by agonists upon extracellular administration may be a result of the latency necessary for membrane permeation. Nonetheless, differential activation of plasmalemmal CB<sub>2</sub> by the three agonists (applied extracellularly) is more likely to be a result of the functional selectivity at CB<sub>2</sub>,<sup>7,34</sup> which is supported by the previous finding that 2-AG (which promotes agonist-directed trafficking at CB<sub>2</sub>)<sup>34</sup> has a low potency at eliciting CB<sub>2</sub>-mediated  $Ca^{2+}$  responses.<sup>34</sup> Binding of a particular agonist to a GPCR results in the enrichment of a unique set of receptor conformations

based on the microaffinity of the agonist for each conformation; because distinct conformations presumably couple receptors differently to specific G proteins and intracellular effectors, individual agonists ultimately produce distinct effects.<sup>11</sup> As such, anandamide, 2-AG, and WIN55,212-2 may induce conformational changes in plasmalemmal CB<sub>2</sub>, resulting in distinct responses, as observed in the study presented here. However, we note that this is not the case with intracellular, endolysosomally located CB<sub>2</sub>, which appears to couple to the same Gq-mediated  $Ca^{2+}$  pathway in response to intracellular administration of the three agonists; moreover, the three agonists have higher potency and efficacy at eliciting intracellularly initiated CB<sub>2</sub>-dependent  $Ca^{2+}$  responses. Thus, functional selectivity may apply more to plasmalemmal than to intracellular CB<sub>2</sub>.

On a different note, plasma membrane-located CB<sub>2</sub> is internalized upon agonist stimulation and slowly recycled back to the cell surface via a Rab11-dependent pathway, while rapid recycling, via Rab4, does not occur.<sup>40</sup> Moreover, in the case of CB<sub>2</sub>, not all receptors are recycled, and chronic agonist stimulation does not promote switching from recycling to degradative pathways, supporting the hypothesis of a putative

role of sequestration of the CB<sub>2</sub> receptor to the cytoplasm following internalization.<sup>40</sup>

Our results, together with those of others,<sup>12</sup> add further complexity to the CB<sub>2</sub> receptor pharmacology and argue for careful consideration of receptor localization in the development of CB<sub>2</sub>-based therapeutic agents. Moreover, because 2-AG is intracellularly produced "on demand",<sup>41</sup> its first target may be intracellularly located CB<sub>2</sub>, which may be relevant both in physiological states and in pathologies with an increased level of production of endocannabinoids.

## ■ ASSOCIATED CONTENT

### S Supporting Information

Evidence of negligible effects of extracellular anandamide on CB<sub>2</sub>-expressing U2OS cells or untransfected U2OS cells, insignificant responses produced by microinjected anandamide in untransfected U2OS cells is provided as supplemental data, and insignificant Ca<sup>2+</sup> responses to extracellular or intracellular administration of WIN55,212-2 in untransfected U2OS cells. This material is available free of charge via the Internet at <http://pubs.acs.org>.

## ■ AUTHOR INFORMATION

### Corresponding Authors

\*Center for Substance Abuse Research, Temple University School of Medicine, 3500 N. Broad St., Room 848, Philadelphia, PA 19140. E-mail: ebrailou@temple.edu. Telephone: (215) 707-2791. Fax: (215) 707-9890.

\*Center for Substance Abuse Research, Temple University School of Medicine, 3500 N. Broad St., Room 852, Philadelphia, PA 19140. E-mail: mabood@temple.edu. Telephone: (215) 707-2638. Fax: (215) 707-6661.

### Author Contributions

G.C.B. and E.D. contributed equally to this work.

### Funding

This work was supported by National Institutes of Health Grants HL090804 (to E.B.) and DA035926 and DA023204 (to M.E.A.).

### Notes

The authors declare no competing financial interests.

## ■ ACKNOWLEDGMENTS

We thank Drs. Marc Caron and Lawrence S. Barak (Duke University) for providing the CB<sub>2</sub>-U2OS cell line and the CB<sub>2</sub>-GFP cDNA.

## ■ ABBREVIATIONS

2-AG, 2-arachidonoyl glycerol; [Ca<sup>2+</sup>]<sub>i</sub>, intracellular Ca<sup>2+</sup> concentration; CB<sub>2</sub>-U2OS, CB<sub>2</sub>-β-arrestin 2-green fluorescent protein-U2OS; CTX, cholera toxin; DMEM, Dulbecco's modified Eagle's medium; D-SP, D-[Trp<sup>7,9,10</sup>]-substance P; EGTA, ethylene glycol tetraacetic acid; GFP, green fluorescent protein; GPCR, G protein-coupled receptor; HBSS, Hank's balanced salt solution; IP<sub>3</sub>R, inositol 1,4,5-trisphosphate receptor; MAPK, mitogen-activated protein kinase; NAADP, nicotinic acid adenine dinucleotide phosphate; PTX, pertussis toxin; RFP, red fluorescent protein.

## ■ REFERENCES

- Pertwee, R. G., Howlett, A. C., Abood, M. E., Alexander, S. P., Di Marzo, V., Elphick, M. R., Greasley, P. J., Hansen, H. S., Kunos, G., Mackie, K., Mechoulam, R., and Ross, R. A. (2010) International Union of Basic and Clinical Pharmacology. LXXIX. Cannabinoid receptors and their ligands: Beyond CB<sub>1</sub> and CB<sub>2</sub>. *Pharmacol. Rev.* 62, 588–5631.
- Anand, P., Whiteside, G., Fowler, C. J., and Hohmann, A. G. (2009) Targeting CB<sub>2</sub> receptors and the endocannabinoid system for the treatment of pain. *Brain Res. Rev.* 60, 255–266.
- Cabral, G. A., and Griffin-Thomas, L. (2009) Emerging role of the cannabinoid receptor CB<sub>2</sub> in immune regulation: Therapeutic prospects for neuroinflammation. *Expert Rev. Mol. Med.* 11, e3.
- Riether, D. (2012) Selective cannabinoid receptor 2 modulators: A patent review 2009–present. *Expert Opin. Ther. Pat.* 22, 495–510.
- Ruhl, T., Deuther-Conrad, W., Fischer, S., Gunther, R., Hennig, L., Krautscheid, H., and Brust, P. (2012) Cannabinoid receptor type 2 (CB<sub>2</sub>)-selective N-aryl-oxadiazolyl-propionamides: Synthesis, radiolabelling, molecular modelling and biological evaluation. *Org. Med. Chem. Lett.* 2, 32.
- Atwood, B. K., and Mackie, K. (2010) CB<sub>2</sub>: A cannabinoid receptor with an identity crisis. *Br. J. Pharmacol.* 160, 467–479.
- Atwood, B. K., Wager-Miller, J., Haskins, C., Straiker, A., and Mackie, K. (2012) Functional selectivity in CB<sub>2</sub> cannabinoid receptor signaling and regulation: Implications for the therapeutic potential of CB<sub>2</sub> ligands. *Mol. Pharmacol.* 81, 250–263.
- Onaivi, E. S., Ishiguro, H., Gu, S., and Liu, Q. R. (2012) CNS effects of CB<sub>2</sub> cannabinoid receptors: Beyond neuro-immuno-cannabinoid activity. *J. Psychopharmacol.* 26, 92–103.
- Liu, Q. R., Pan, C. H., Hishimoto, A., Li, C. Y., Xi, Z. X., Llorente-Berzal, A., Viveros, M. P., Ishiguro, H., Arinami, T., Onaivi, E. S., and Uhl, G. R. (2009) Species differences in cannabinoid receptor 2 (CNR2 gene): Identification of novel human and rodent CB<sub>2</sub> isoforms, differential tissue expression and regulation by cannabinoid receptor ligands. *Genes Brain Behav.* 8, 519–530.
- Bingham, B., Jones, P. G., Uveges, A. J., Kotnis, S., Lu, P., Smith, V. A., Sun, S. C., Resnick, L., Chlenov, M., He, Y., Strassle, B. W., Cummons, T. A., Piesla, M. J., Harrison, J. E., Whiteside, G. T., and Kennedy, J. D. (2007) Species-specific in vitro pharmacological effects of the cannabinoid receptor 2 (CB<sub>2</sub>) selective ligand AM1241 and its resolved enantiomers. *Br. J. Pharmacol.* 151, 1061–1070.
- Urban, J. D., Clarke, W. P., von Zastrow, M., Nichols, D. E., Kobilka, B., Weinstein, H., Javitch, J. A., Roth, B. L., Christopoulos, A., Sexton, P. M., Miller, K. J., Spedding, M., and Mailman, R. B. (2007) Functional selectivity and classical concepts of quantitative pharmacology. *J. Pharmacol. Exp. Ther.* 320, 1–13.
- den Boon, F. S., Chameau, P., Schaafsma-Zhao, Q., van Aken, W., Bari, M., Oddi, S., Kruse, C. G., Maccarrone, M., Wadman, W. J., and Werkman, T. R. (2012) Excitability of prefrontal cortical pyramidal neurons is modulated by activation of intracellular type-2 cannabinoid receptors. *Proc. Natl. Acad. Sci. U.S.A.* 109, 3534–3539.
- De Petrocellis, L., Marini, P., Matias, I., Moriello, A. S., Starowicz, K., Cristino, L., Nigam, S., and Di Marzo, V. (2007) Mechanisms for the coupling of cannabinoid receptors to intracellular calcium mobilization in rat insulinoma β-cells. *Exp. Cell Res.* 313, 2993–3004.
- Sugiura, T., Kondo, S., Kishimoto, S., Miyashita, T., Nakane, S., Kodaka, T., Suhara, Y., Takayama, H., and Waku, K. (2000) Evidence that 2-arachidonoylglycerol but not N-palmitoylethanolamine or anandamide is the physiological ligand for the cannabinoid CB<sub>2</sub> receptor. Comparison of the agonistic activities of various cannabinoid receptor ligands in HL-60 cells. *J. Biol. Chem.* 275, 605–612.
- Zoratti, C., Kipmen-Korgun, D., Osibow, K., Malli, R., and Graier, W. F. (2003) Anandamide initiates Ca<sup>2+</sup> signaling via CB<sub>2</sub> receptor linked to phospholipase C in calf pulmonary endothelial cells. *Br. J. Pharmacol.* 140, 1351–1362.
- Yu, J., Deliu, E., Zhang, X. Q., Hoffman, N. E., Carter, R. L., Grisanti, L. A., Brailou, G. C., Mades, M., Cheung, J. Y., Force, T., Abood, M. E., Koch, W. J., Tilley, D. G., and Brailou, E. (2013) Differential Activation of Cultured Neonatal Cardiomyocytes by Plasmalemmal Versus Intracellular G Protein-coupled Receptor 55. *J. Biol. Chem.* 288, 22481–22492.

- (17) Brailoiu, G. C., Oprea, T. I., Zhao, P., Aboot, M. E., and Brailoiu, E. (2011) Intracellular cannabinoid type 1 (CB1) receptors are activated by anandamide. *J. Biol. Chem.* 286, 29166–29174.
- (18) Deliu, E., Brailoiu, G. C., Eguchi, S., Hoffman, N. E., Rabinowitz, J. E., Tilley, D. G., Madesh, M., Koch, W. J., and Brailoiu, E. (2014) Direct evidence of intracrine angiotensin II signaling in neurons. *Am. J. Physiol.* 306, C736–C744.
- (19) Deliu, E., Brailoiu, G. C., Mallikaraman, K., Wang, H., Madesh, M., Undieh, A. S., Koch, W. J., and Brailoiu, E. (2012) Intracellular endothelin type B receptor-driven  $\text{Ca}^{2+}$  signal elicits nitric oxide production in endothelial cells. *J. Biol. Chem.* 287, 41023–41031.
- (20) Grynkiewicz, G., Poenie, M., and Tsien, R. Y. (1985) A new generation of  $\text{Ca}^{2+}$  indicators with greatly improved fluorescence properties. *J. Biol. Chem.* 260, 3440–3450.
- (21) Bowman, E. J., Siebers, A., and Altendorf, K. (1988) Bafilomycins: A class of inhibitors of membrane ATPases from microorganisms, animal cells, and plant cells. *Proc. Natl. Acad. Sci. U.S.A.* 85, 7972–7976.
- (22) Kunz, J. B., Schwarz, H., and Mayer, A. (2004) Determination of four sequential stages during microautophagy in vitro. *J. Biol. Chem.* 279, 9987–9996.
- (23) Wang, T., Ming, Z., Xiaochun, W., and Hong, W. (2011) Rab7: Role of its protein interaction cascades in endo-lysosomal traffic. *Cell. Signalling* 23, 516–521.
- (24) Mukai, H., Munekata, E., and Higashijima, T. (1992) G protein antagonists. A novel hydrophobic peptide competes with receptor for G protein binding. *J. Biol. Chem.* 267, 16237–16243.
- (25) Naylor, E., Arredouani, A., Vasudevan, S. R., Lewis, A. M., Parkesh, R., Mizote, A., Rosen, D., Thomas, J. M., Izumi, M., Ganesan, A., Galione, A., and Churchill, G. C. (2009) Identification of a chemical probe for NAADP by virtual screening. *Nat. Chem. Biol.* 5, 220–226.
- (26) Jalink, K., and Moolenaar, W. H. (2010) G protein-coupled receptors: The inside story. *BioEssays* 32, 13–16.
- (27) Zhu, T., Gobeil, F., Vazquez-Tello, A., Leduc, M., Rihakova, L., Bossolasco, M., Bkaily, G., Peri, K., Varma, D. R., Orvoine, R., and Chemtob, S. (2006) Intracrine signaling through lipid mediators and their cognate nuclear G-protein-coupled receptors: A paradigm based on PGE2, PAF, and LPA1 receptors. *Can. J. Physiol. Pharmacol.* 84, 377–391.
- (28) Benard, G., Massa, F., Puente, N., Lourenco, J., Bellocchio, L., Soria-Gomez, E., Matias, I., Delamarre, A., Metna-Laurent, M., Cannich, A., Hebert-Chatelin, E., Mulle, C., Ortega-Gutierrez, S., Martin-Fontech, M., Klugmann, M., Guggenhuber, S., Lutz, B., Gertsch, J., Chaoulloff, F., Lopez-Rodriguez, M. L., Grandes, P., Rossignol, R., and Marsicano, G. (2012) Mitochondrial CB<sub>1</sub> receptors regulate neuronal energy metabolism. *Nat. Neurosci.* 15, 558–564.
- (29) Howlett, A. C., Barth, F., Bonner, T. I., Cabral, G., Casellas, P., Devane, W. A., Felder, C. C., Herkenham, M., Mackie, K., Martin, B. R., Mechoulam, R., and Pertwee, R. G. (2002) International Union of Pharmacology. XXVII. Classification of cannabinoid receptors. *Pharmacol. Rev.* 54, 161–202.
- (30) Glass, M., and Felder, C. C. (1997) Concurrent stimulation of cannabinoid CB1 and dopamine D2 receptors augments cAMP accumulation in striatal neurons: Evidence for a G<sub>s</sub> linkage to the CB1 receptor. *J. Neurosci.* 17, 5327–5333.
- (31) Lauckner, J. E., Hille, B., and Mackie, K. (2005) The cannabinoid agonist WIN55,212-2 increases intracellular calcium via CB1 receptor coupling to Gq/11 G proteins. *Proc. Natl. Acad. Sci. U.S.A.* 102, 19144–19149.
- (32) Sugiura, T., Kodaka, T., Kondo, S., Nakane, S., Kondo, H., Waku, K., Ishima, Y., Watanabe, K., and Yamamoto, I. (1997) Is the cannabinoid CB1 receptor a 2-arachidonoylglycerol receptor? Structural requirements for triggering a  $\text{Ca}^{2+}$  transient in NG108-15 cells. *J. Biochem.* 122, 890–895.
- (33) Sugiura, T., Kodaka, T., Kondo, S., Tonegawa, T., Nakane, S., Kishimoto, S., Yamashita, A., and Waku, K. (1996) 2-Arachidonoylglycerol, a putative endogenous cannabinoid receptor ligand, induces rapid, transient elevation of intracellular free  $\text{Ca}^{2+}$  in neuroblastoma x glioma hybrid NG108-15 cells. *Biochem. Biophys. Res. Commun.* 229, 58–64.
- (34) Shoemaker, J. L., Ruckle, M. B., Mayeux, P. R., and Prather, P. L. (2005) Agonist-directed trafficking of response by endocannabinoids acting at CB2 receptors. *J. Pharmacol. Exp. Ther.* 315, 828–838.
- (35) Irannejad, R., Tomshine, J. C., Tomshine, J. R., Chevalier, M., Mahoney, J. P., Steyaert, J., Rasmussen, S. G., Sunahara, R. K., El-Samad, H., Huang, B., and von Zastrow, M. (2013) Conformational biosensors reveal GPCR signalling from endosomes. *Nature* 495, 534–538.
- (36) Deliu, E., Tica, A. A., Motoc, D., Brailoiu, G. C., and Brailoiu, E. (2011) Intracellular angiotensin II activates rat myometrium. *Am. J. Physiol.* 301, C559–C565.
- (37) Cosker, F., Cheviron, N., Yamasaki, M., Menteyne, A., Lund, F. E., Moutin, M. J., Galione, A., and Cancela, J. M. (2010) The ectoenzyme CD38 is a nicotinic acid adenine dinucleotide phosphate (NAADP) synthase that couples receptor activation to  $\text{Ca}^{2+}$  mobilization from lysosomes in pancreatic acinar cells. *J. Biol. Chem.* 285, 38251–38259.
- (38) Kim, S. Y., Cho, B. H., and Kim, U. H. (2010) CD38-mediated  $\text{Ca}^{2+}$  signaling contributes to angiotensin II-induced activation of hepatic stellate cells: Attenuation of hepatic fibrosis by CD38 ablation. *J. Biol. Chem.* 285, 576–582.
- (39) Davis, L. C., Morgan, A. J., Ruas, M., Wong, J. L., Graeff, R. M., Poustka, A. J., Lee, H. C., Wessel, G. M., Parrington, J., and Galione, A. (2008)  $\text{Ca}^{2+}$  signaling occurs via second messenger release from intraorganelle synthesis sites. *Curr. Biol.* 18, 1612–1618.
- (40) Grimsey, N. L., Goodfellow, C. E., Dragunow, M., and Glass, M. (2011) Cannabinoid receptor 2 undergoes Rab5-mediated internalization and recycles via a Rab11-dependent pathway. *Biochim. Biophys. Acta* 1813, 1554–1560.
- (41) Hashimotodani, Y., Ohno-Shosaku, T., Tanimura, A., Kita, Y., Sano, Y., Shimizu, T., Di Marzo, V., and Kano, M. (2013) Acute inhibition of diacylglycerol lipase blocks endocannabinoid-mediated retrograde signalling: Evidence for on-demand biosynthesis of 2-arachidonoylglycerol. *J. Physiol.* 591, 4765–4776.